HHS Public Access

Author manuscript

Hear Res. Author manuscript; available in PMC 2017 May 01.

Published in final edited form as:

Hear Res. 2016 May ; 335: 64–75. doi:10.1016/j.heares.2016.02.013.

Graded and discontinuous EphA-ephrinB expression patterns in the developing auditory brainstem

Matthew M. Wallace[1], **J. Aaron Harris**[1], **Donald Q. Brubaker**[1], **Caitlyn A. Klotz**[1], and **Mark L. Gabriele**[1]

[1]James Madison University Department of Biology Harrisonburg, VA 22807, USA

Abstract

Eph-ephrin interactions guide topographic mapping and pattern formation in a variety of systems. In contrast to other sensory pathways, their precise role in the assembly of central auditory circuits remains poorly understood. The auditory midbrain, or inferior colliculus (IC) is an intriguing structure for exploring guidance of patterned projections as adjacent subdivisions exhibit distinct organizational features. The central nucleus of the IC (CNIC) and deep aspects of its neighboring lateral cortex (LCIC, Layer 3) are tonotopically-organized and receive layered inputs from primarily downstream auditory sources. While less is known about more superficial aspects of the LCIC, its inputs are multimodal, lack a clear tonotopic order, and appear discontinuous, terminating in modular, patch/matrix-like distributions. Here we utilize X-Gal staining approaches in *lacZ* mutant mice (ephrin-B2, -B3, and EphA4) to reveal EphA-ephrinB expression patterns in the nascent IC during the period of projection shaping that precedes hearing onset. We also report early postnatal protein expression in the cochlear nuclei, the superior olivary complex, the nuclei of the lateral lemniscus, and relevant midline structures. Continuous ephrin-B2 and EphA4 expression gradients exist along frequency axes of the CNIC and LCIC Layer 3. In contrast, more superficial LCIC localization is not graded, but confined to a series of discrete ephrin-B2 and EphA4-positive Layer 2 modules. While heavily expressed in the midline, much of the auditory brainstem is devoid of ephrin-B3, including the CNIC, LCIC Layer 2 modular fields, the dorsal nucleus of the lateral lemniscus (DNLL), as well as much of the superior olivary complex and cochlear nuclei. Ephrin-B3 LCIC expression appears complementary to that of ephrin-B2 and EphA4, with protein most concentrated in presumptive extramodular zones. Described tonotopic gradients and seemingly complementary modular/extramodular patterns suggest Eph-ephrin guidance in establishing juxtaposed continuous and discrete neural maps in the developing IC prior to experience.

[*]Mail Correspondence to: Dr. Mark L. Gabriele, Ph.D., Professor, James Madison University, Department of Biology, MSC 7801, 951 Carrier Drive, Harrisonburg, Virginia 22807, phone: (540) 568-6333, fax: (540) 568-3333, gabrieml@jmu.edu.

CONFLICT OF INTEREST STATEMENT

The authors declare all research was conducted in the absence of any commercial or financial relationships that could be construed as a potential conflict of interest.

Keywords

ephrin; Eph receptor; topography; inferior colliculus; superior olivary complex; cochlear nucleus; lateral lemniscus

1. INTRODUCTION

Centrally located in the mesencephalon, the inferior colliculus (IC) receives a complex combination of extrinsic inputs (Winer and Schreiner, 2005) amongst a dense network of intrinsic connections (Sturm et al., 2014). Projections from a host of auditory nuclei converge on its central nucleus (CNIC), terminating in a tonotopic manner as afferent layers that extend along its laminar continuum and into deep aspects of the neighboring lateral cortex (LCIC, Layer 3). In contrast to these primarily auditory areas, more superficial LCIC regions are multimodal and lack a clear frequency order (Aitkin et al., 1981; Gruters and Groh, 2012). In lieu of layers or fibrodendritic flaminae, a series of neurochemically-distinct modules define the multimodal LCIC (Mugnaini and Oertel, 1985; Chernock et al., 2004; Lesicko and Llano, 2015) with afferents preferentially targeting Layer 2 modular fields or surrounding extramodular domains. While not fully characterized, patterned inputs to these areas include auditory projections from the dorsal cochlear nucleus (Shore and Zhou, 2006; Zhou and Shore, 2006), the CNIC (Saldaña and Merchán, 1992; Noftz et al., 2014), and auditory cortex (Saldaña et al., 1996; Torii et al., 2013; Stebbings et al., 2014; Barnstedt et al, 2015), as well as a diverse array arising from nonauditory sources (Olazábal and Moore, 1989; Shammah-Lagnado et al., 1996), including somatosensory projections from the spinal trigeminal (Sp5, Shore and Zhou, 2006; Zhou and Shore, 2006) and dorsal column nuclei (Li and Mizuno, 1997).

Previously, we demonstrated that topographic layered inputs to the CNIC emerge prior to experience in a variety of species (Gabriele et al., 2000a, b; Henkel et al., 2005; Gabriele et al., 2007; Fathke and Gabriele, 2009; Gabriele et al., 2011; Wallace et al., 2013). Distinct axonal plexuses are evident by postnatal day 4 (P4) and exhibit highly refined adult-like projection patterns by hearing onset (P12, in rat and mouse). The early spatial alignment of alternating and partially overlapping layered inputs provides evidence that highly precise CNIC maps form in the absence of experience (Fathke and Gabriele, 2009). While less is known about LCIC circuit assembly, preliminary findings from our laboratory suggest a similar accuracy in initial targeting of multimodal discontinuous modular/extramodular fields (Noftz et al., 2014; Balsamo and Gabriele, 2015).

The Eph-ephrin signaling family fulfills all criteria for topographic guidance molecules (McLaughlin and O'Leary 2005) and is well-documented for its instructive role in the establishment of two kinds of neural maps, *continuous* and *discrete* (Luo and Flanagan, 2007). Eph-ephrin gradients provide positional information necessary for continuous maps that preserve nearest neighbor relationships from source to target (e.g. retinotectal multiaxes mapping: Triplett and Feldheim, 2012). Discontinuous or segregated Eph-ephrin expression, on the other hand, is consistent with discrete mapping, whereby connections are arranged according to input type as opposed to spatial position (e.g. striosome/matrix map: Gerfen,

1992; Janis et al., 1999, olfactory glomerular map; Strotmann and Breer, 2006). Typically, auditory maps are categorized as continuous with their emphasis on tonotopic order and preservation of cochlear place code. Tonotopic gradients of Eph family proteins at various levels suggest their involvement in constructing orderly frequency-specific circuits (Person et al., 2004; Miko et al., 2007; Gabriele et al., 2011). Manipulations of certain Eph-ephrin members indeed affect *in vivo* mapping of tonotopic circuits at the level of the auditory brainstem (Cramer, 2005; Huffman and Cramer, 2007; Nakamura et al., 2012; Wallace et al., 2013) and even shape aspects of cortical auditory response properties (Intskirveli et al., 2011). Even with this recent progress, considerable work remains in identifying the full spectrum of signaling members, expression gradients, and mechanisms that drive continuous auditory map formation. Multimodal targets like LCIC modular/extramodular fields exhibit unique organizational features, and thus, appear more in keeping with discrete neural maps (Cramer and Gabriele, 2014). The presence of both continuous and discrete maps within a single system would not be unprecedented, given the somatosensory system's respective elements of body surface representation and whisker-specific barreloids/barrel fields.

Functional roles for ephrin-B2, -B3 and EphA4 in aspects of the developing auditory system downstream of the IC have been previously reported in the literature (Bianchi and Gale, 1998; Pickles et al., 2002; Brors et al., 2003; Cramer, 2005; Miko et al, 2007; Defourny et al., 2013), although less is known about their expression and involvement in midbrain mapping (Gabriele et al., 2011; Wallace et al., 2013; Cramer and Gabriele, 2014). Transgenic lines with *lacZ* reporter gene manipulations in coding regions of Eph-ephrin genes of interest provide the means for mapping endogenous gene expression in developing auditory structures of animals carrying a mutant allele (Bianchi et al., 2002; Miko et al., 2007; Miko et al., 2008). The present expression study provides the first step in exploring the notion that continuous and discrete guidance maps exist juxtaposed in neighboring IC subdivisions. Quantification of X-Gal staining in *lacZ* mutants reveals clear EphA4 and ephrin-B2 gradients in the tonotopic CNIC and LCIC Layer 3. Within the multimodal LCIC, periodic modular (ephrin-B2, EphA4) and extramodular (ephrin-B3) expression patterns appear complementary. Despite belonging to different Eph-ephrin subfamilies, EphA4 has strong binding affinities for both ephrin-A and ephrin-B ligands (Gale et al., 1996; Pasquale, 1997; Bergemann et al., 1998). Expression patterns are also noted for other major auditory brainstem nuclei and relevant midline structures. The potential instructive role of the described graded and modular expression patterns in establishing continuous tonotopic and discrete multimodal neural maps within the CNIC and LCIC are discussed.

2. MATERIALS AND METHODS

2.1. Animal subjects

Early postnatal mice (P0, P4, P8, P12) were studied leading up to hearing onset (P12). Timepoints were chosen to directly correlate with stages from previous studies documenting the development of multiple topographic and patterned inputs to the IC (Gabriele et al., 2000a, 2000b, 2007, 2011; Henkel et al., 2005; Fathke and Gabriele, 2009; Wallace et al., 2013). Results include data from 36 heterozygous mice of three different Eph-ephrin *lacZ* mutations (ephrin-B2, CD1/129 background, n = 19; EphA4, C57BL/6J background, n = 8;

ephrin-B3, CD1 background n = 9). Breeding pairs for ephrin-B2 and ephrin-B3 colonies were provided by Dr. Mark Henkemeyer; EphA4 colony was generated from breeding pairs acquired from the Mutant Mouse Regional Resource Center (MMRRC, NCRR-NIH; donated by Marc Tessier-Lavigne). *LacZ* insertions afford β-galactosidase or X-Gal histochemical staining (5-bromo-4-chloro-3-indolyl-β-D-galactopyranoside; X-Gal, Sigma-Aldrich, St. Louis, MO), faithfully reporting gene expression for the proteins of interest. Positive X-Gal staining results in a blue reaction product for visualization with brightfield microscopy.

Visualized β-galactosidase in our mutant strains results from *lacZ* reporter gene manipulations in coding regions for the genes of interest. In the ephrin-B2 and -B3 strains, mutant alleles encode for membrane-bound ephrin-B2 (or -B3) - β-galactosidase fusion proteins in which the cytoplasmic domain has been deleted and replaced with β-gal (Dravis et al., 2004). Affixing β-gal to truncated ephrin-B2 or ephrin-B3 enables precise spatial and subcellular visualization of these proteins (Yokoyama et al., 2001). In contrast, the mutant allele for the EphA4 gene trap strain produces no EphA4 protein and expresses cytoplasmic β-galactosidase (Leighton et al., 2001).

2.2. Genotyping procedures

Ephrin-B2 mice were genotyped as previously described (Gabriele et al., 2011; Wallace et al., 2013). Similar methods were employed for EphA4 and ephrin-B3 genotyping. In short, EphA4 and ephrin-B3 tail samples were digested, isolated, and precipitated with an Easy-DNA kit (Invitrogen, Carlsbad, CA). EphA4 (EphA4-forward 5′ GTTTCCGCTCTGAGCTTATACTGC-3′, EphA4-reverse 5′ ACAGTGAGTGGACAAAGAGACAGG-3′, lacZ 5′-CGCTCTTACCAAAGGGCAAACC-3′) and ephrin-B3 primers (EB3-forward 5′-GACGGCGGGCCAAGCCTTCGGAGAG -3′, EB3-reverse 5′-ATAGCCAGGAGGAGCCAAAGAG-3′, lacZ 5′-AGGCGATTAAGTTGGGTAACG-3′) were used for PCR amplification (Dravis et al., 2004; Miko et al., 2007). Visualization of PCR product via gel electrophoresis results in EphA4 wild-type (WT; 639-bp) and/or mutant (800-bp) allele bands, and ephrin-B3 WT (401-bp) and/or mutant (142-bp) allele bands. All experimental procedures were performed in compliance with the National Institutes of Health Guide for the Care and Use of Laboratory Animals (NIH Publications No. 80-23, revised 1996) and received prior approval from the Institutional Animal Care and Use Committee at James Madison University (Gabriele IACUC Protocol No. A14-15).

2.3. X-Gal staining

Following an overdose of ketamine (200 mg/kg) and xylazine (20 mg/kg) ephrin-B2$^{lacZ/+}$, EphA4$^{lacZ/+}$, and ephrin-B3$^{lacZ/+}$ heterozygous mice were perfused with physiological rinse followed by 4% paraformaldehyde fixative (pH 7.4). Following perfusion, brains were immediately cryoprotected in 30% sucrose solution at 4°C. Once equilibrated, brains were blocked, sectioned on a sliding freezing microtome at 50 μm, and mounted on gelatin-subbed slides. Slides were transferred to mailers with 2% paraformaldehyde solution at 4°C for five minutes, and then rinsed twice for ten minutes at 4°C in PBS with 2mM $MgCl_2$. Slides were then incubated in the dark in a final X-Gal working solution pre-warmed to

37°C (5 mM potassium ferricyanide, 5 mM potassium ferrocyanide, 2 mM Mg Cl_2, and 1 mg/mL X-Gal, Sigma-Aldrich, St. Louis, MO). After 24 hours at 37°C, slides were rinsed for five minutes in PBS, transferred into 4% paraformaldehyde for five minutes, and then rinsed again in PBS for five minutes. Sections were dehydrated with increasing EtOH concentrations and cleared in three successive xylene steps at ten minute intervals. Sections were coverslipped with DPX mountant (Sigma-Aldrich, St. Louis, MO).

It is worth noting that initial X-Gal staining attempts included an overnight postfixing step prior to cryoprotection. Although never explicitly stated in the literature to our knowledge, we noticed that every case processed with an overnight postfix yieled no significant X-Gal staining, while ommission or substantial abbreviation of this step (10 minute postfix) consistently resulted in a robust and reliable reaction. Wild-type tissue reliably lacked any *lacZ* reactivity, even when left in working solution for 72 hours.

2.4. Microscopy and image acquisition

Brightfield images were captured on a Nikon C1si system (Nikon Eclipse TE2000-E, Nikon, Melville, NY) using a Nikon Digital Sight DS-U2 color camera. Image acquisition was conducted utilizing NIS-Elements Software (Nikon). Captured images were white balanced and raw image data files were saved as uncompressed TIFFs for quantification purposes. Images were modified slightly for brightness and contrast for consistency purposes (Adobe Photoshop, San Jose, CA). Nuclear boundaries were determined paying attention to regional variations in cellular packing densities. Darkfield microscopy was also utilized to reveal fibrous layers and aid in delineating LCIC lamination.

2.5. Sampling of graded and modular expression pattern plot profiles

Quantitative CNIC gradient data was compiled and grouped to facilitate comparisons between two established early postnatal periods of projection shaping. The two earlier timepoints (P0/P4) were grouped as they correspond to the initial period of axonal invasion and elaboration within the IC. Similarly, the latter timepoints (P8/P12) were grouped as this period leading up to hearing onset coincides with axonal pattern formation within the developing IC (Gabriele et al., 2011). For quantification, raw uncompressed TIFFs were imported into ImageJ software (NIH, Bethesda, MD). A 2σ-factor Gaussian blur was applied to each image following conversion to an 8-bit grayscale in ImageJ. For CNIC sampling, representative images from mid-rostrocaudal aspects of the CNIC were rotated approximately 45° to facilitate sampling along its tonotopic axis. A rectangular sampling box was drawn and positioned accordingly to cover the entirety of the frequency axis. Brightness profile values generated from each sampling were plotted as a function of distance across the CNIC. For every distance (x) along the sampling area, the corresponding single column of grayscale data were averaged to calculate the brightness profile value (y). Normalized values were calculated by dividing brightness values corresponding to every x-value (distance) by the average brightness value for each respective case. Each case's normalized values were plotted against their distance within both age groups to form compiled graphs in Excel (Microsoft Corporation, Redmond, WA). Linear regressions were performed on nornalized plot profiles. A set criteria for graded expressions was defined as those having a slope greater than 1.0×10^{-04}.

A freehand tool in ImageJ set to a line thickness of 20 pixels was used to draw curved contours for sampling LCIC Layer 2 and 3 image data. Each was sampled from ventral to dorsal, bisecting presumptive Layer 2 modules or traversing the tontopic axis of Layer 3. Unless tissue quality warranted fewer, a minimum of three sections were sampled that were representative of each protein's rostrocaudal IC expression.

3. RESULTS

3.1. Graded and modular ephrin-B2 and EphA4 IC expression patterns

X-Gal staining reveals graded ephrin-B2 and EphA4 expression in the tonotopic CNIC and LCIC Layer 3 during the early postnatal period of projection shaping leading up to hearing onset (Fathke and Gabriele, 2009; Gabriele et al., 2011; Wallace et al., 2013). Sampling along the frequency axis of the CNIC yields continuous gradients, with each protein most concentrated in ventromedial, high-frequency regions (Fig. 1A–D). The similarly layered and tonotopically organized LCIC Layer 3 (Saldaña and Merchán, 1992, Loftus et al., 2008) exhibits comparable ephrin-B2 and EphA4 gradients, with strong expression ventrally in high frequency areas that diminishes dorsally in lower frequency domains (Fig. 1A, B; E, F).

A contrasting discontinuous expression pattern is observed for both ephrin-B2 and EphA4 in LCIC Layer 2 (Fig. 2A, B, *dashed contours*) during the same developmental period. Sampling along the curved LCIC Layer 2 contour in each case generates brightness plot profiles that consistently highlight this periodic modular distribution (Fig. 2C, D, *arrows*). Discrete expression modules, while absent from caudal extremes of the LCIC, are distinct at mid-rostrocaudal levels and extend into rostral aspects of the LCIC.

3.2. Ephrin-B3 expression localized to LCIC extramodular zones

Unlike ephrin-B2 and EphA4, ephrin-B3 is conspicuously absent from the CNIC (Fig. 3A–C). Sampling along the CNIC frequency axis yields no evidence of a graded expression and consistently low levels of X-Gal labeling (Fig. 3B). LCIC Layer 2 modules are likewise devoid of ephrin-B3 (Fig. 3A, C), whereas neuropil in presumptive surrounding extramodular zones is distinctly positive. Curved contour sampling bisecting LCIC Layer 2 modular fields (Fig. 3C) reliably emphasizes the discontinuous periodic pattern of ephrin-B3 negative patches (Fig. 3D, *arrows).* The dorsal cortex of the IC (DCIC) exhibits ephrin-B3 expression levels comparable to that of LCIC extramodular zones. Fibers coursing through aspects of the IC commissure into the DCIC are distinctly ephrin-B3 positive (Fig 3A, C, *arrowheads; see also* Fig. 9C).

Periodic and discrete EphA/ephrinB expression fields are clearly delineated by P8. Ephrin-B2 and EphA4 expression is restricted to Layer 2 modules (Fig. 4A, B), while ephrin-B3 extramodular labeling appears complementary, with hollow areas of expression in presumptive modular zones embedded within a surrounding network of homogeneous Layer 1 and 3 neuropil labeling (Fig. 4C). Higher magnification reveals ephrin-B2 cellular and neuropil labeling that is almost exclusively confined to Layer 2 modules (Fig. 4A). Despite evidence of labeled somata and neuropil throughout Layer 3 as well as in intermodular gaps of Layer 2, EphA4 staining is similarly most concentrated in Layer 2 modular domains and

equally sparse in fibrous aspects of Layer 1 (Fig. 4B). The consistent cellular appearance of EphA4 LCIC labeling apparent with X-Gal staining methods, however, was not observed in previous immuncytochemical findings from our lab that showed more fibrous EphA4 staining in age-matched animals (Gabriele et al., 2011). This discrepancy might be explained by the fact that our null EphA4 mutant produces no protein, thereby only expressing cytoplasmic β-galactosidase. Beyond seemingly complementary patterns, ephrin-B3 staining differed from that of EphA4 and ephrin-B2 in that there was little evidence of positively-labeled cell bodies throughout the CNIC and its surrounding shell nuclei (Fig. 3A, C; Fig. 4C).

3.3. CNIC gradients at two early postnatal periods of projection shaping

Plots of normalized CNIC data were compiled and organized into two developmental groups (Fig. 5) corresponding to known periods of axonal invasion/elaboration (P0, P4, Kandler and Friauf, 1993; Gabriele et al., 2000a, b; Fathke and Gabriele, 2009) and subsequent refinement (P8, P12; Gabriele et al., 2000a, b; Fathke and Gabriele, 2009; Wallace et al., 2013). According to our set linear regression slope criteria, significant CNIC gradients were consistently observed for both ephrin-B2 (Fig 5A, B; n = 11, n = 8; $m = 4 \times 10^{-04}$, $m = 5 \times 10^{-04}$ respectively) and EphA4 (Fig 5C, D; n = 3, n = 5; $m = 9 \times 10^{-04}$, $m = 7 \times 10^{-04}$ respectively) at each defined developmental category. Slopes of linear regressions for multiple ephrin-B3 cases were negligible during both periods, supporting the observation that this protein is largely absent from the CNIC leading up to hearing onset (Fig. 5E, F; n = 4, n = 5; $m = -5 \times 10^{-05}$, $m = 1 \times 10^{-05}$ respectively).

3.4. Additional auditory brainstem nuclei and midline structure expression

Ventral and dorsal cochlear nuclei (VCN, DCN) expression patterns are dissimilar for ephrin-B2, EphA4, and ephrin-B3 during the first postnatal week. Ephrin-B2 is uniformly expressed throughout the VCN and DCN at P4, showing no gradient along its ventrodorsal frequency axis (Fig. 6A, B). The superficial molecular layer, in contrast, is distinctly negative for ephrin-B2. X-Gal histochemistry in EphA4$^{lacZ/+}$ mutants was not homogeneous, but rather graded in the VCN and DCN during this same developmental period. EphA4 expression is most concentrated in dorsal, high-frequency aspects, as compared to lower expression in more ventral, low frequency regions (Fig. 6C, D, *white arrows*; plot profiles not shown). Findings for ephrin-B2 and EphA4 are consistent with that previously reported by Miko et al. (2007). Ephrin-B3 expression is not graded, but complementary to that of ephrin-B2. Ephrin-B3 is absent from VCN and DCN, except for the molecular layer that is consistently positive (Fig 6E, F).

Many of the principal nuclei of the superior olivary complex (SOC) and surrounding periolivary nuclei exhibit early postnatal EphA/ephrinB expression. During the first postnatal week, ephrin-B2 expression (Fig. 7A) appears uniform in the lateral superior olive (LSO), superior paraolivary nucleus (SPON), medial nucleus of the trapezoid body (MNTB), and dorsal periolivary nucleus (DPO). While lacking from DPO, homogeneous EphA4 expression (Fig. 7B) is also observed in the LSO, SPON, and MNTB, as well as the medioventral and lateroventral periolivary nuclei (MVPO, LVPO). During this same

developmental period leading up to hearing onset, ephrin-B3 is largely absent from the SOC (Fig. 7C).

The nuclei of the lateral lemniscus exhibit varied expression patterns for ephrin-B2, EphA4, and ephrin-B3. While ephrin-B2 is strongly expressed in the ventral nucleus of the lateral lemniscus (VNLL, see Gabriele et al., 2011), its expression in the dorsal nucleus of the lateral lemniscus is comparatively moderate (DNLL, Fig. 8A). EphA4, on the other hand, is most heavily concentrated in the DNLL (Fig. 8B). The DNLL is completely devoid of ephrin-B3, as are fibers of the lateral lemniscus and commissure of Probst (Fig. 8C, *arrowheads*).

Eph-ephrin interactions are known to play a role in midline decisions in a variety of sensory systems (Cramer et al., 2002; Williams et al., 2004; Petros et al., 2008). Ephrin-B2 is expressed along the dorsal midline where colliculo-collicular fibers cross (Fig. 9A, *arrow*), whereas EphA4 is absent here, as well as in the ventral tegmental midline (Fig. 9B, *arrow*). Ephrin-B3 exhibits the most concentrated midline expression during this early developmental period (Fig. 9C, *arrow*) and is also present in intercollicular fibers crossing in the IC commissure (Fig. 9C, *arrowhead*).

4. DISCUSSION

By utilizing X-Gal staining in *lacZ* mutants, the present study reveals continuous and discrete Eph-ephrin IC expression maps during the postnatal period leading up to hearing onset. Coincident with shaping of topographic afferents along tonotopic IC dimensions (Brunso-Bechtold and Henkel, 2005), ephrin-B2 and EphA4 gradients span CNIC and LCIC Layer 3 frequency axes, with protein most concentrated in high-frequency domains. Inputs to more superficial aspects of the LCIC, however, are multimodal (Aitkin et al., 1981; Gruters and Groh, 2012) and discontinuous, exhibiting either discrete modular or extramodular terminal fields (Saldaña and Merchán, 1992; Saldaña et al., 1996; Shore and Zhou, 2006; Torii et al., 2013; Stebbings et al., 2014). These highly localized afferent arrangements share a striking resemblance to modular (ephrin-B2, EphA4) and extramodular (ephrin-B3) LCIC expression patterns presented here. In sum, this study provides a necessary foundation for defining the precise alignment of developing auditory brainstem connections with Eph-ephrin expression patterns, and ultimately determining their role in guiding frequency-specific (continuous) and multimodal (discrete) circuits in the nascent IC.

4.1. Support for LCIC compartmentalized architecture

Compared to the extensive detail that exists concerning the CNIC, its cytoarchitecture, and its well-described afferent and efferent pathways (Oliver, 2005), considerably less is known about analogous LCIC features. A series of neurochemical staining experiments in adult rat and mouse provide preliminary insights about its presumed compartmentalized organization. Periodic LCIC Layer 2 neuronal clusters or modules are clearly evident after immuno- and histochemical staining for parvalbumin, cytochrome oxidase, nicotinamide adenine dinucleotide phosphate-diaphorase, and acetylcholinesterase (Chernock et al., 2004; Lesicko and Llano, 2015). Surrounding extramodular domains while negative for these markers, are strikingly positive for calretinin in developing rat (Lohmann and Friauf, 1996).

Here we provide guidance molecule expression data in developing mouse that underscores the notion of a compartmentalized LCIC. EphA4 and ephrin-B2 are expressed in discrete patches in LCIC Layer 2, while ephrin-B3 expression is consistently extramodular in its appearance. These expression patterns are evident by birth and persist during the early postnatal period preceding hearing onset. The seemingly complementary patterns of EphA4/ephrin-B2 and ephrin-B3 labeling appear to correlate nicely not only with the aforementioned neurochemical LCIC substrate, but also with multimodal innervation of these areas. LCIC receives ascending inputs from somatosensory centers including the dorsal column and spinal trigeminal nuclei (Li and Mizuno, 1997; Zhou and Shore, 2006) that preferentially terminate as a series of discontinuous patches spanning Layer 2. LCIC afferents also arise from the ipsilateral and contralateral CNIC (Saldaña and Merchán, 1992), as well as descending projections from auditory cortex (Coleman and Clerici, 1987; Druga et al., 1997; Torii et al., 2013). These intracollicular, colliculocollicular, and corticocollicular inputs putatively target LCIC zones surrounding the described “patchy” Layer 2 substrate. Furthermore, studies in the adult rat describe patchy GABAergic output modules (Mugnaini and Oertel, 1985) that target the auditory thalamus, with particularly strong connections to the neighboring posterior limitans and posterior intralaminar nuclei (PLi and PIN, Saldaña, 2013). Elucidating specific afferent-efferent circuits and directly correlating their development with LCIC Eph-ephrin expression patterns will be instrumental in uncovering mechanisms responsible for shaping the three-dimensional LCIC mosaic architecture.

4.2. Continuous and discrete maps in the developing IC?

Continuous CNIC and LCIC Layer 3 gradients along defined frequency axes are reminiscent of those observed in the developing visual system across target tectal anterior-posterior dimensions (McLaughlin and O’Leary, 2005; Suetterlin et al., 2012). In the analogous optic tectum or superior colliculus, countergradients of EphAs and ephrin-As control aspects of retinotectal topographic mapping and axonal branching patterns. While both ephrin-B2 and EphA4 expression in tonotopic regions of the IC exhibit consistent gradients, additional Eph-ephrins are also present and likely influential during this early period of projection shaping (Fig. 10). Similar trends of ephrin-B2, EphA4, and ephrin-B3 expression are observed downstream of the IC, in that ephrin-B2 and EphA4 are highly expressed as compared to minimal ephrin-B3 expression. While EphA4 cochlear nuclear expression exhibits a gradient matching that of the IC, most nuclei in the SOC and lateral lemniscal nuclei positive for EphA4 and/or ephrin-B2 were ostensibly homogeneous in their expression. It remains to be seen which other members of the Eph-ephrin family are present in downstream sources of input to the IC, and whether corresponding presynaptic expression molecules exhibit matching or countergradients to those described in the tonotopic IC. Such findings might suggest chemoattractive/repellent mechanisms working in tandem for establishing frequency-specific circuits in the IC prior to experience. Indeed, coupling of permissive and repulsive mechanisms are integral in the establishment of retinotectal topography (McLaughlin and O’Leary, 2005), as one drives patterning in the anterior-posterior axis (repulsive, EphAs/ephrin-As), while the other instructs medial-lateral mapping (attractive; EphBs/ephrinBs). Perhaps an analogous system exists in the CNIC and LCIC Layer 3 such that gradients like those presented here help provide positional information

along the tonotopic axis, while other gradients yet to be discovered instruct targeting of specific fibrodendritic functional zones in the rostrocaudal dimension.

Unlike the tonotopic CNIC and LCIC Layer 3, graded expressions do not prevail in other aspects of the LCIC, but rather a mosaic architecture of modular and extramodular domains. Such a periodic arrangement of complementary expression patterns is reminiscent of that seen in several other systems. In early olfactory glomerular development terminal fields are guided through EphA-ephrinA interactions (Vassar et al., 1994; St. John et al., 2002). The compartmentalized LCIC modular Layer 2 arrangement also harkens back to EphA-ephrinA interactions and patterning of somatosensory cortical barrel fields (Garel and Rubenstein, 2004; Vanderhaeghen and Polleux, 2004; Uziel et al., 2006). LCIC modular organization, its multimodal connections, and its role in sensorimotor reflexes may most closely parallel that of the striatum and its EphA-ephrinA dependent signaling for the segregation of striatal projection neurons into patch/matrix functional compartments (Janis et al., 1999; Passante et al., 2008).

4.3. CNIC vs. LCIC: An intriguing developmental model

The LCIC and its innervation scheme differ considerably from the CNIC. In addition to compartmentalized terminal fields that integrate ascending information, the LCIC also receives descending cortical influences as well as extramodal inputs from the somatosensory system. The LCIC thus shares many characteristics with the similarly compartmentalized and neurochemically-distinct intermediate/deep layers of the multisensory superior colliculus (SC; Jeon and Mize, 1993; Graybiel and Illing, 1994; Gabriele et al., 2006). Multisensory integration encoded here requires the precise alignment of developing visual, auditory, and somatosensory maps. This spatial registry appears to involve both space-matching mechanisms for same-system inputs, whereby relative levels of spontaneous activity achieve retinocollicular and corticollicular alignment (Triplett et al., 2009), as well as activity-independent mechanisms (EphA-ephrinA interactions) for multimodal alignments (descending somatosensory mapping within deep SC; Triplett et al., 2012). It seems plausible that the developing LCIC may employ an analogous combination of endogenous activity and guidance-matching mechanisms for driving its functional architecture that also ensures accurate orientation and reflexive behaviors.

4.4. Eph-ephrin expression in midline structures

In our examination of developing auditory nuclei we noted complementary expression patterns in both tectal and tegmental midline structures (Fig. 9). These findings are of particular interest given the sheer number of crossed auditory projections at the level of the IC and below. Ephrin-B2, -B3 are heavily expressed at the midline, in contrast to EphA4 which is notably absent here. It is likely that Eph-ephrin midline expression is involved in midline decisions for crossed and uncrossed auditory fibers. Additional studies are needed to discern whether this midline expression is transient, how it correlates with the time course of known crossing fibers, and the potential interactions Eph-ephrins may have with various transcription factors and midline radial glia as is the case for crossing decisions in other systems (e.g. optic chiasm; Petros et al., 2008).

4.5. Conclusion

With new developmental resources such as comprehensive *in situ* hybridization databases (Fig. 10, www.brainmap.org), it is clear that additional Eph-ephrin members play a role in the complex puzzle of interactions that shape both topographic and patterned arrangements in the developing IC. With its rich array of inputs, each perhaps with its own unique Eph-ephrin expression patterns, considerable work remains to uncover the precise mechanisms that instruct fine-structure targeting of CNIC frequency layers (Schreiner and Langer 1997; Gabriele et al., 2000b; Fathke and Gabriele, 2009) and LCIC modular/extramodular fields. Taken together, the IC provides a promising model for study of both continuous (CNIC and LCIC Layer 3) and discrete (LCIC Layer 2) map formation in a single structure. Future experiments that directly address how established developmental blueprints translate into mature auditory and multisensory functional maps are needed.

Acknowledgments

This work was supported by the National Institutes of Health (DC012421-01) and the National Science Foundation (DBI-0619207). The authors also thank Dr. Mark Henkemeyer and the Mutant Mouse Regional Resource Centers (MMRRC) for their help generating the Eph-ephrin lines, Dr. Thomas Gabriele for his guidance with statistical analyses, and Devon Cowan for programming of quantitative ImageJ macros.

References

Aitkin LM, Kenyon CE, Philpott P. The representation of the auditory and somatosensory systems in the external nucleus of the cat inferior colliculus. J Comp Neurol. 1981; 196:25–40. [PubMed: 7204665]

Balsamo JA, Gabriele ML. Somatosensory inputs to the lateral cortex of the inferior colliculus prior to experience in mouse. Assoc Res Otolaryng Mtg. 2015:PS-565.

Barnstedt O, Keating P, Weissenberger Y, King AJ, Dahmen JC. Functional Microarchitecture of the Mouse Dorsal Inferior Colliculus Revealed through In Vivo Two-Photon Calcium Imaging. J Neurosci. 2015; 35:10927–39. [PubMed: 26245957]

Bianchi LM, Dinsio K, Davoli K, Gale NW. Lac z histochemistry and immunohistochemistry reveal ephrin-B ligand expression in the inner ear. J Histochem Cytochem. 2002; 50:1641–5. [PubMed: 12486086]

Bianchi LM, Gale NW. Distribution of Eph-related molecules in the developing and mature cochlea. Hear Res. 1998; 117:161–172. [PubMed: 9557986]

Bergemann AD, Zhang L, Chiang MK, Brambilla R, Klein R, Flanagan JG. Ephrin-B3, a ligand for the receptor EphB3, expressed at the midline of the developing neural tube. Oncogene. 1998; 16:471–480. [PubMed: 9484836]

Brors D, Bodmer D, Pak K, Aletsee C, Schäfers M, Dazert S, Ryan AF. EphA4 provides repulsive signals to developing cochlear ganglion neurites mediated through ephrin-B2 and -B3. J Comp Neurol. 2003; 462:90–100. [PubMed: 12761826]

Brunso-Bechtold, JK.; Henkel, CK. Development of auditory afferents to the central nucleus of the inferior colliculus. In: Winer, JA.; Schreiner, CE., editors. The Inferior Colliculus. New York: Springer; 2005. p. 537-558.

Chernock ML, Larue DT, Winer JA. A periodic network of neurochemical modules in the inferior colliculus. Hear Res. 2004; 188:12–20. [PubMed: 14759566]

Coleman JR, Clerici WJ. Sources of projections to subdivisions of the inferior colliculus in the rat. J Comp Neurol. 1987; 262:215–226. [PubMed: 3624552]

Cramer KS. Eph proteins and the assembly of auditory circuits. Hear Res. 2005; 206:42–51. [PubMed: 16080997]

Cramer KS, Gabriele ML. Axon guidance in the auditory system: Multiple functions of Eph receptors. Neurosci. 2014; 277:152–162.

Cramer KS, Karam SD, Bothwell M, Cerretti DP, Pasquale EB, Rubel EW. Expression of EphB receptors and EphrinB ligands in the developing chick auditory brainstem. J Comp Neurol. 2002; 452:51–64. [PubMed: 12205709]

Defourny J, Poirrier AL, Lallemend F, Mateo Sanchez S, Neef J, Vanderhaeghen P, Soriano E, Peuckert C, Kullander K, Fritzsch B, Nguyen L, Moonen G, Moser T, Malgrange B. Ephrin- A5/EphA4 signalling controls specific afferent targeting to cochlear hair cells. Nat Commun. 2013; 4:1438. [PubMed: 23385583]

Dravis C, Yokoyama N, Chumley MJ, Cowan CA, Silvany RE, Shay J, Baker LA, Henkemeyer M. Bidirectional signaling mediated by ephrin-B2 and EphB2 controls urorectal development. Dev Biol. 2004; 271:272–290. [PubMed: 15223334]

Druga R, Syka J, Rajkowska G. Projections of auditory cortex onto the inferior colliculus in the rat. Physiol Res. 1997; 46:215–222. [PubMed: 9728510]

Fathke RL, Gabriele ML. Patterning of multiple layered projections to the auditory midbrain prior to experience. Hear Res. 2009; 249:36–43. [PubMed: 19271271]

Gabriele ML, Brubaker DQ, Chamberlain KA, Kross KM, Simpson NS, Kavianpour SM. EphA4 and ephrin-B2 expression patterns during inferior colliculus projection shaping prior to experience. Dev Neurobiol. 2011; 71:182–199. [PubMed: 20886601]

Gabriele ML, Brunso-Bechtold JK, Henkel CK. Development of afferent patterns in the inferior colliculus of the rat: projection from the dorsal nucleus of the lateral lemniscus. J Comp Neurol. 2000a; 416:368–382. [PubMed: 10602095]

Gabriele ML, Brunso-Bechtold JK, Henkel CK. Plasticity in the development of afferent patterns in the inferior colliculus of the rat after unilateral cochlear ablation. J Neurosci. 2000b; 20:6939–6949. [PubMed: 10995838]

Gabriele ML, Shahmoradian SH, French CC, Henkel CK, McHaffie JG. Early segregation of layered projections from the lateral superior olivary nucleus to the central nucleus of the inferior colliculus in the neonatal cat. Brain Res. 2007; 1173:66–77. [PubMed: 17850770]

Gabriele ML, Smoot JE, Jiang H, Stein BE, McHaffie JG. Early establishment of adult-like nigrotectal architecture in the neonatal cat: a double-labeling study using carbocyanine dyes. Neurosci. 2006; 137:1309–1319.

Gale NW, Holland SJ, Valenzuela DM, Flenniken A, Pan L, Ryan TE, Henkemeyer M, Strebhardt K, Hirai H, Wilkinson DG, Pawson T, Davis S, Yancopoulos GD. Eph receptors and ligands comprise two major specificity subclasses and are reciprocally compartmentalized during embryogenesis. Neuron. 1996; 19:9–19. [PubMed: 8755474]

Garel S, Rubenstein JL. Intermediate targets in formation of topographic projections: inputs from the thalamocortical system. Trends Neurosci. 2004; 27:533–539. [PubMed: 15331235]

Gerfen CR. The neostriatal mosaic: multiple levels of compartmental organization in the basal ganglia. Annu Rev Neurosci. 1992; 15:285–320. [PubMed: 1575444]

Graybiel AM, Illing RB. Enkephalin-positive and acetylcholinesterase-positive patch systems in the superior colliculus have matching distributions but distinct developmental histories. J Comp Neurol. 1994; 340:297–310. [PubMed: 8188852]

Gruters KG, Groh JM. Sounds and beyond: multisensory and other non-auditory signals in the inferior colliculus. Front Neural Circuits. 2012 Dec 11.6:96.10.3389/fncir.2012.00096 [PubMed: 23248584]

Henkel CK, Gabriele ML, McHaffie JG. Quantitative assessment of developing afferent patterns in the cat inferior colliculus revealed with calbindin immunohistochemistry and tract tracing methods. Neurosci. 2005; 136:945–955.

Huffman KJ, Cramer KS. EphA4 misexpression alters tonotopic projections in the auditory brainstem. Dev Neurobiol. 2007; 67:1655–1668. [PubMed: 17577206]

Intskirveli I, Metherate R, Cramer KS. Null mutations in EphB receptors decrease sharpness of frequency tuning in primary auditory cortex. PLoS One. 2011; 6:e26192. [PubMed: 22022561]

Janis LS, Cassidy RM, Kromer LF. Ephrin-A binding of EphA receptor expression delineate the matrix compartment of the striatum. J Neurosci. 1999; 19:4962–4971. [PubMed: 10366629]

Jeon CJ, Mize RR. Choline acetyltransferase-immunoreactive patches overlap specific efferent cell groups in the cat superior colliculus. J Comp Neurol. 1993; 337:127–150. [PubMed: 8276989]

Kandler K, Friauf E. Pre- and postnatal development of efferent connections of the cochlear nucleus in the rat. J Comp Neurol. 1993; 328:161–84. [PubMed: 8423239]

Leighton PA, Mitchell KJ, Goodrich LV, Lu X, Pinson K, Scherz P, Skarnes WC, Tessier-Lavigne M. Defining brain wiring patterns and mechanisms through gene trapping in mice. Nature. 2001; 410:174–9. [PubMed: 11242070]

Lesicko AMH, Llano DA. Connectional and neurochemical modularity of the mouse inferior colliculus. Assoc Res Otolaryng Mtg. 2015:PS-564.

Li H, Mizuno N. Single neurons in the spinal trigeminal and dorsal column nuclei project to both the cochlear nucleus and the inferior colliculus by way of axon collaterals: a fluorescent retrograde double-labeling study in the rat. Neurosci Res. 1997; 29:135–142. [PubMed: 9359462]

Loftus WC, Malmierca MS, Bishop DC, Oliver DL. The cytoarchitecture of the inferior colliculus revisisted: A common organization of the lateral cortex in rat and cat. Neurosi. 2008; 154:196–205.

Lohmann C, Friauf E. Distribution of the calcium-binding proteins parvalbumin and calretinin in the auditory brainstem of adult and developing rats. J Comp Neurol. 1996; 367:90–109. [PubMed: 8867285]

Luo L, Flanagan JG. Development of continuous and discrete neural maps. Neuron. 2007; 56:284–300. [PubMed: 17964246]

McLaughlin T, O'Leary DD. Molecular gradients and development of retinotopic maps. Annu Rev Neurosci. 2005; 28:327–355. [PubMed: 16022599]

Miko IJ, Nakamura PA, Henkemeyer M, Cramer KS. Auditory brainstem neural activation patterns are altered in EphA4- and ephrin-B2-deficient mice. J Comp Neurol. 2007; 505:669–681. [PubMed: 17948875]

Miko IJ, Henkemeyer M, Cramer KS. Auditory brainstem responses are impaired in EphA4 and ephrin-B2 deficient mice. Hear Res. 2008; 235:39–46. [PubMed: 17967521]

Mugnaini, E.; Oertel, WH. An atlas of the distribution of GABAergic neurons and terminals in the rat CNS as revealed by GAD immunocytochemistry. In: Björklund, A.; Hökfelt, T., editors. Handbook of Chemical Neuroanatomy. Amsterdam, Netherlands: Elsevier Science; 1985. p. 436-608.

Nakamura PA, Hsieh CY, Cramer KS. EphB signaling regulates target innervation in the developing and deafferented auditory brainstem. Dev Neurobiol. 2012; 72:1243–55. [PubMed: 22021100]

Noftz WA, Gray LC, Gabriele ML. Converging midbrain afferent patterns and auditory brainstem responses in ephrin-B3 mutant mice. Assoc Res Otolaryng Mtg. 2014:PS-070.

Olazábal UE, Moore JK. Nigrotectal projection to the inferior colliculus: horseradish peroxidase, transport and tyrosine hydroxylase immunohistochemical studies in rats, cats, and bats. J Comp Neurol. 1989; 282:98–118. [PubMed: 2565350]

Oliver, DL. Neuronal organization in the inferior colliculus. In: Winer, JA.; Schreiner, CE., editors. The Inferior Colliculus. New York: Springer; 2005. p. 69-114.

Pasquale EB. The Eph family of receptors. Curr Opin Cell Biol. 1997; 9:608–615. [PubMed: 9330863]

Passante L, Gaspard N, Degraeve M, Frisén J, Kullander K, De Maertelaer V, Vanderhaeghen P. Temporal regulation of ephrin/Eph signalling is required for the spatial patterning of the mammalian striatum. Development. 2008; 135:3281–3290. [PubMed: 18755772]

Person AL, Cerretti DP, Pasquale EB, Rubel EW, Cramer KS. Tonotopic gradients of Eph family proteins in the chick nucleus laminaris during synaptogenesis. J Neurobiol. 2004; 60:28–39. [PubMed: 15188270]

Petros TJ, Rebsam A, Mason CA. Retinal axon growth at the optic chiasm: to cross or not to cross. Annu Rev Neurosci. 2008; 31:295–315. [PubMed: 18558857]

Pickles JO, Claxton C, Van Heumen WR. Complementary and layered expression of Ephs and ephrins in developing mouse inner ear. J Comp Neurol. 2002; 449:207–216. [PubMed: 12115675]

Saldaña E. Ascending projections to the non-lemniscal auditory thalamus. Assoc Res Otolaryngol Mtg. 2013:856.

Saldaña E, Feliciano M, Mugnaini E. Distribution of descending projections from primary auditory neocortex to inferior colliculus mimics the topography of intracollicular projections. J Comp Neurol. 1996; 37:15–40. [PubMed: 8835717]

Saldaña E, Merchán MA. Intrinsic and commissural connections of the rat inferior colliculus. J Comp Neurol. 1992; 319:417–437. [PubMed: 1376335]

Schreiner CE, Langner G. Laminar fine structure of frequency organization in auditory midbrain. Nature. 1997; 388:383–386. [PubMed: 9237756]

Shammah-Lagnado SJ, Alheid GF, Heimer L. Efferent connections of the caudal part of the globus pallidus in the rat. J Comp Neurol. 1996; 376:489–507. [PubMed: 8956113]

Shore S, Zhou J. Somatosensory influence on the cochlear nucleus and beyond. Hear Res. 2006; 216–217:90–99.

Stebbings KA, Lesicko AM, Llano DA. The auditory corticocollicular system: molecular and circuit-level considerations. Hear Res. 2014; 314:51–59. [PubMed: 24911237]

St John JA, Pasquale EB, Key B. EphA receptors and ephrin-A ligands exhibit highly regulated spatial and temporal expression patterns in the developing olfactory system. Brain Res Dev Brain Res. 2002; 138:1–14. [PubMed: 12234653]

Strotmann J, Breer H. Formation of glomerular maps in the olfactory system. Semin Cell Dev Biol. 2006; 17:402–410. [PubMed: 16807005]

Sturm J, Nguyen T, Kandler K. Development of intrinsic connectivity in the central nucleus of the mouse inferior colliculus. J Neurosci. 2014; 34:15032–46. [PubMed: 25378168]

Suetterlin P, Marler KM, Drescher U. Axonal ephrinA/EphA interactions, and the emergence of order in topographic projections. Semin Cell Dev Biol. 2012; 23:1–6. [PubMed: 22040913]

Torii M, Hackett TA, Rakic P, Levitt P, Polley DB. EphA signaling impacts development of topographic connectivity in auditory corticofugal systems. Cereb Cortex. 2013; 23:775–785. [PubMed: 22490549]

Triplett JW, Feldheim DA. Eph and ephrin signaling in the formation of topographic maps. Semin Cell Dev Biol. 2012; 23:7–15. [PubMed: 22044886]

Triplett JW, Owens MT, Yamada J, Lemke G, Cang J, Stryker MP, Feldheim DA. Retinal input instructs alignment of visual topographic maps. Cell. 2009; 139:175–185. [PubMed: 19804762]

Triplett JW, Phan A, Yamada J, Feldheim DA. Alignment of multimodal sensory input in the superior colliculus through a gradient-matching mechanism. J Neurosci. 2012; 32:5264–5271. [PubMed: 22496572]

Uziel D, Garcez P, Lent R, Peuckert C, Niehage R, Weth F, Bolz J. Connecting thalamus and cortex: the role of ephrins. Anat Rec A Discov Mol Cell Evol Biol. 2006; 288:135–142. [PubMed: 16411249]

Vanderhaeghen P, Polleux F. Developmental mechanisms patterning thalamocortical projections: intrinsic, extrinsic and in between. Trends in Neurosci. 2004; 27:384–391.

Vassar R, Chao SK, Sitcheran R, Nuñez JM, Vosshall LB, Axel R. Topographic organization of sensory projections to the olfactory bulb. Cell. 1994; 79:981–991. [PubMed: 8001145]

Wallace MM, Kavianpour SM, Gabriele ML. Ephrin-B2 reverse signaling is required for topography but not pattern formation of lateral superior olivary inputs to the inferior colliculus. J Comp Neurol. 2013; 521:1585–1597. [PubMed: 23042409]

Williams SE, Mason CA, Herrera E. The optic chiasm as a midline choice point. Curr Opin Neurobiol. 2004; 14:51–60. [PubMed: 15018938]

Winer, JA.; Schreiner, CE. The central auditory systems: A functional analysis. In: Winer, JA.; Schreiner, CE., editors. The Inferior Colliculus. New York: Springer; 2005. p. 1-60.

Yokoyama N, Romero MI, Cowan CA, Galvan P, Helmbacher F, Charnay P, Parada LF, Henkemeyer M. Forward signaling mediated by ephrin-B3 prevents contralateral corticospinal axons from recrossing the spinal cord midline. Neuron. 2001; 29:85–97. [PubMed: 11182083]

Zhou J, Shore S. Convergence of spinal trigeminal and cochlear nucleus projections in the inferior colliculus of the guinea pig. J Comp Neurol. 2006; 495:100–112. [PubMed: 16432905]

Highlights

- Eph-ephrin involvement in IC mapping events prior to experience is proposed.
- Tonotopic regions of the mouse IC exhibit graded EphA4 and ephrin-B2 expression.
- Discrete Eph-ephrin patterns define multimodal aspects of the lateral cortex (LCIC).
- EphA4/ephrin-B2 LCIC modules contrast extramodular ephrin-B3 expression.
- The findings provide a guidance substrate resembling nascent IC afferent patterns.

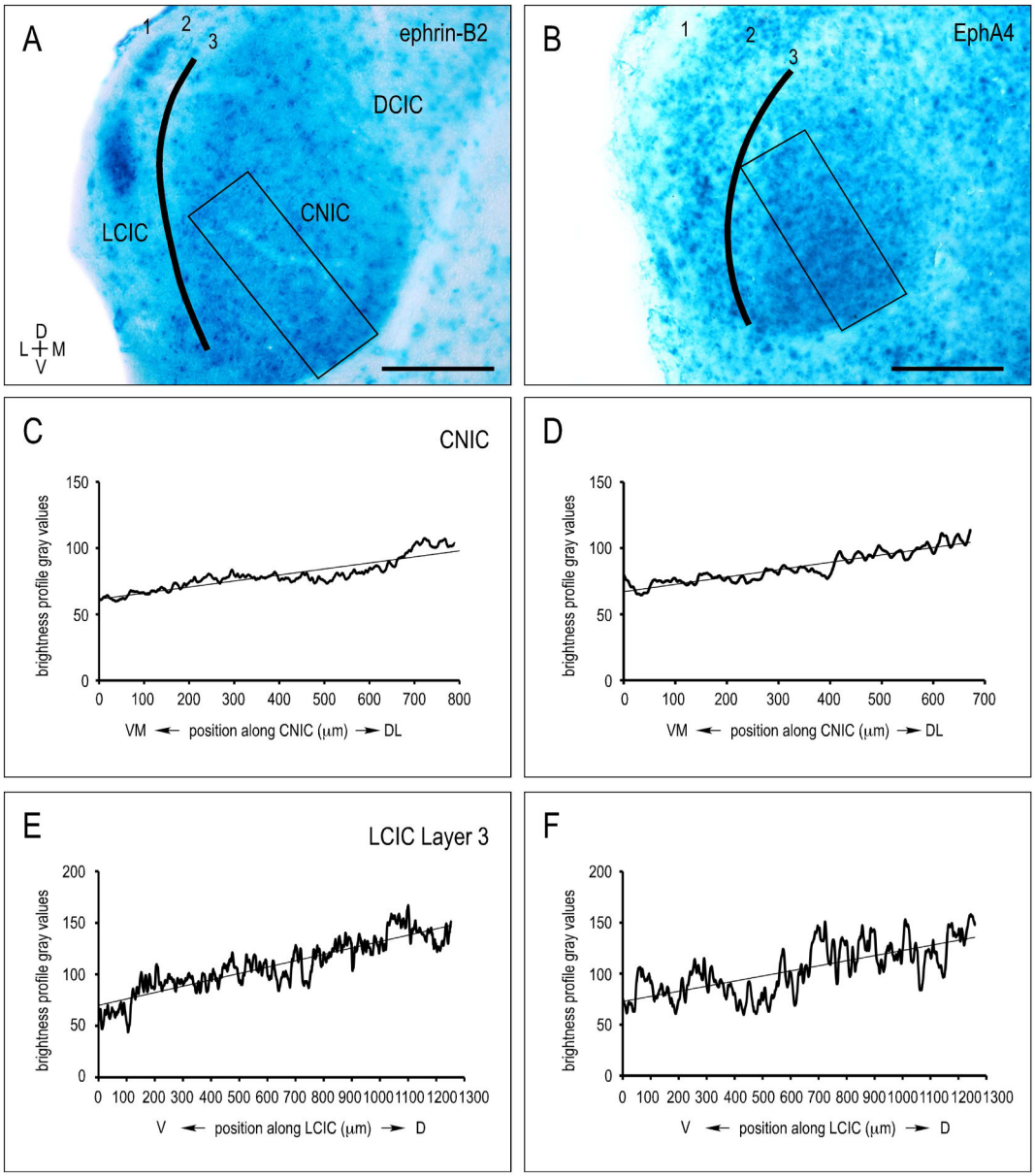

Figure 1.

Early neonatal IC X-Gal labeling for ephrin-B2 (A) and EphA4 (B) at P8. Brightness profiles generated via *rectangular* (CNIC; C, D) and *curved contour* (LCIC Layer 3; E, F) sampling using ImageJ software. Areas of high protein expression and dark reaction product yield lower brightness values, whereas regions with low protein expression and less X-Gal staining correspond to higher brightness values. Linear regressions show similar slopes/gradients in ephrin-B2 (C) and EphA4 (D) CNIC expression. LCIC Layer 3 brightness plots reveal ephrin-B2 (E) and EphA4 (F) gradients comparable to those observed in the CNIC. In both instances, expression gradients followed known frequency axes (CNIC: ventromedial-to-dorsolateral, LCIC Layer 3: ventral-to-dorsal), with protein levels most concentrated in high-frequency regions. Scale bars = 200 μm.

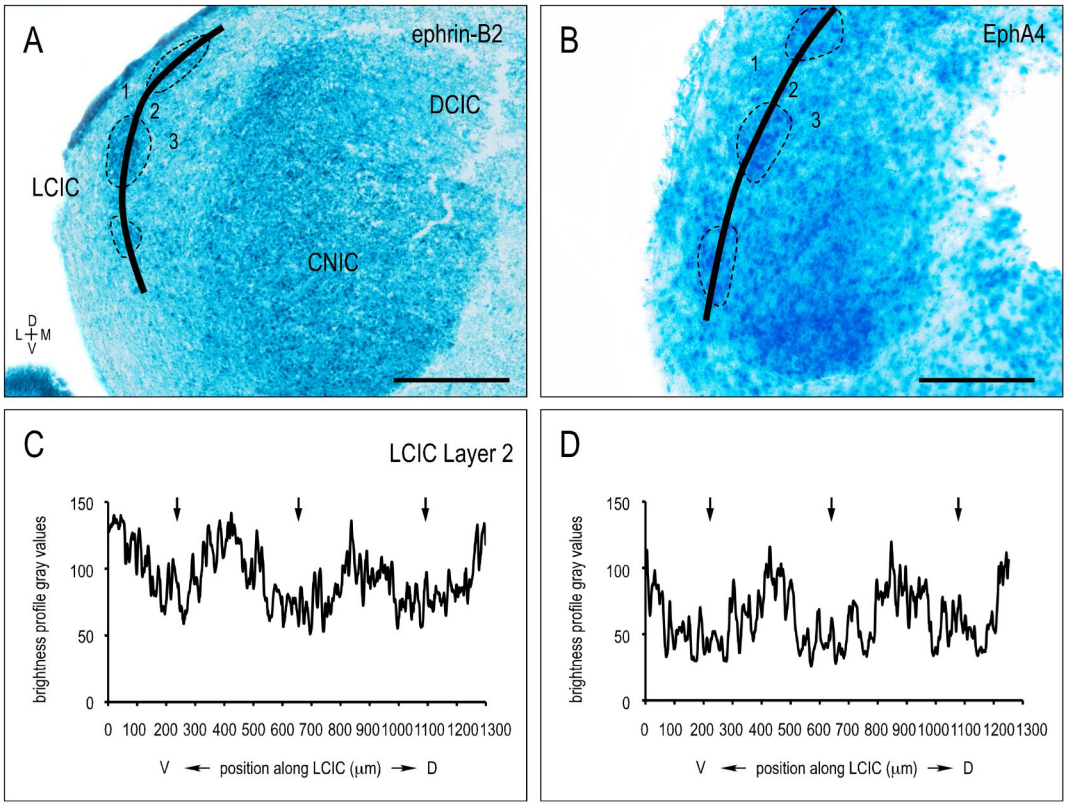

Figure 2.

Discontinuous ephrin-B2 (A) and EphA4 (B) LCIC Layer 2 expression during the first postnatal week (P8). Curved sampling through LCIC Layer 2 (*solid contours* in A, B) reveals periodic ephrin-B2 and EphA4 modules (*dashed contours* in A, B; corresponding *arrows* in C, D plot profiles). Scale bars = 200 μm.

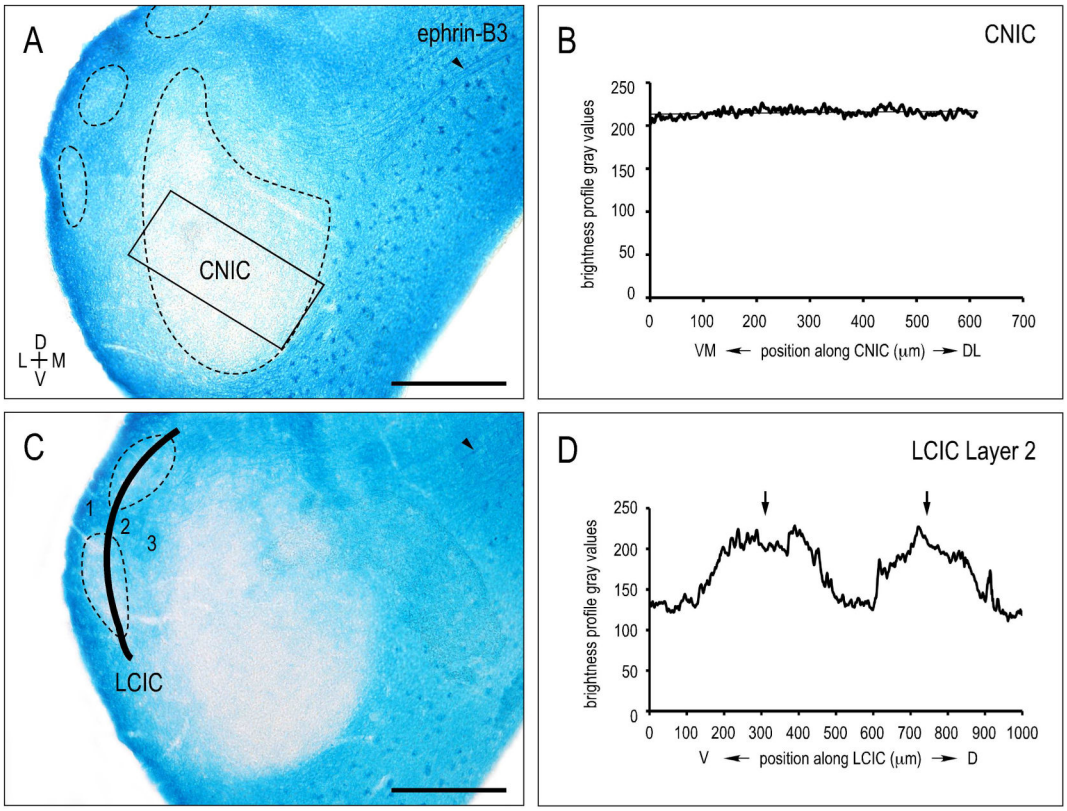

Figure 3.

CNIC (A) and LCIC Layer 2 (C) ephrin-B3 X-Gal labeling at P8 with corresponding brightness profiles (B, D; respectively). Rectangular sampling and linear regression analysis of CNIC (B) show an absence of ephrin-B3 protein prior to hearing onset. While positive in extramodular regions, curved contour sampling along LCIC Layer 2 reveal distinct ephrin-B3-negative modules (*arrows* in D). Ephrin-B3 positive fibers are apparent coursing through the IC commisure (*arrowheads* in A, C). Scale bars = 200 μm.

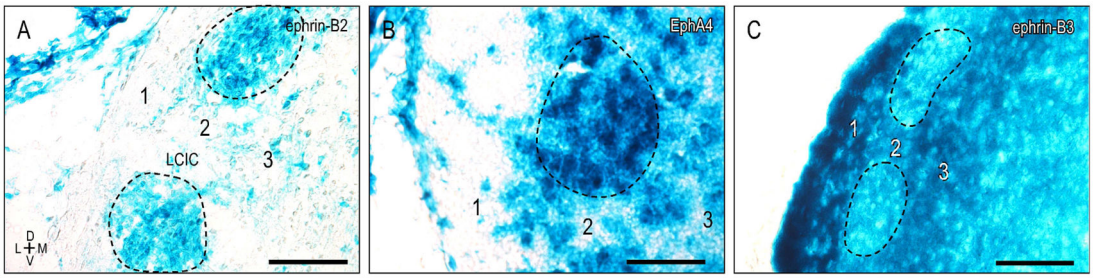

Figure 4.

Higher magnification LCIC expression of ephrin-B2 (A) EphA4 (B) and ephrin-B3 (C) at P8. Ephrin-B2 and EphA4 expression includes somata and neuropil labeling that is most heavily concentrated within periodic, discontinuous presumptive modular fields (A, B, *dashed contours*). In contrast, ephrin-B3 labeling is low in presumptive modular zones (C, *dashed* contours) and more uniformly distributed in surrounding extramodular domains. Scale bars = 50 μm.

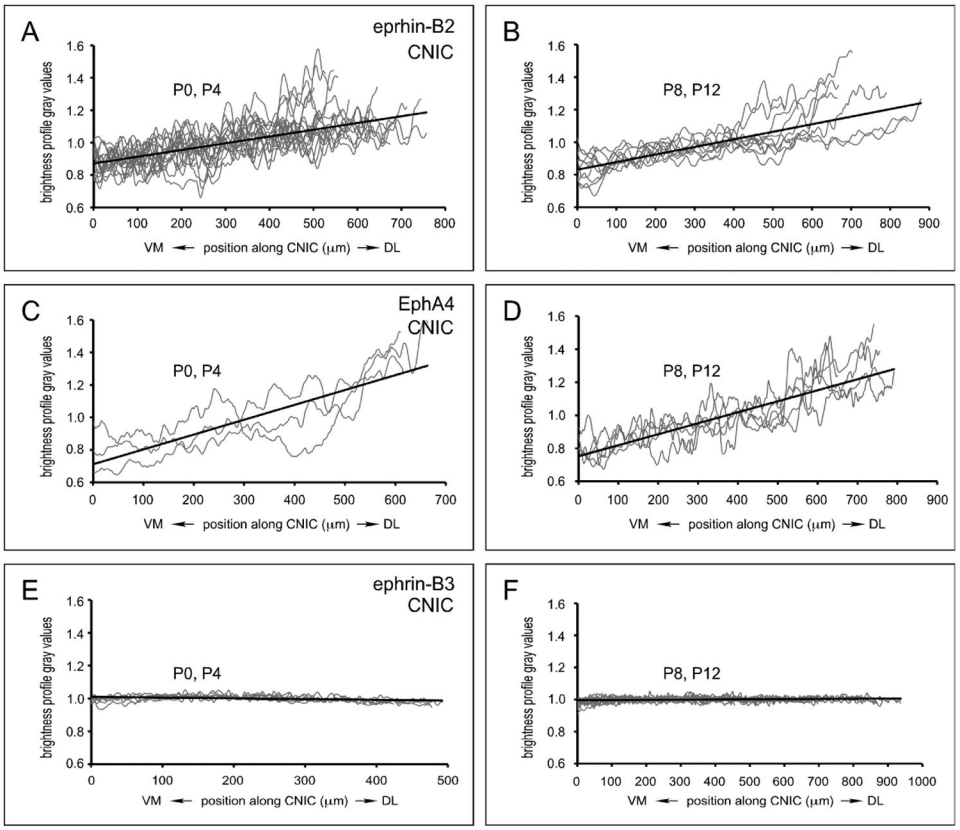

Figure 5.

Normalized linear regression plots of CNIC expression for compiled ephrin-B2 (A, B), EphA4 (C, D), and ephrin-B3 (E, F) data. Plots were grouped into two developmental categories (P0/P4: A, C, E and P8/P12: B, D, F). Clear CNIC gradients are observed for both ephrin-B2 (A, B) and EphA4 (C, D) at each of the defined developmental pairings. In contrast, ephrin-B3 (E, F) is conspicuously absent from the nascent CNIC.

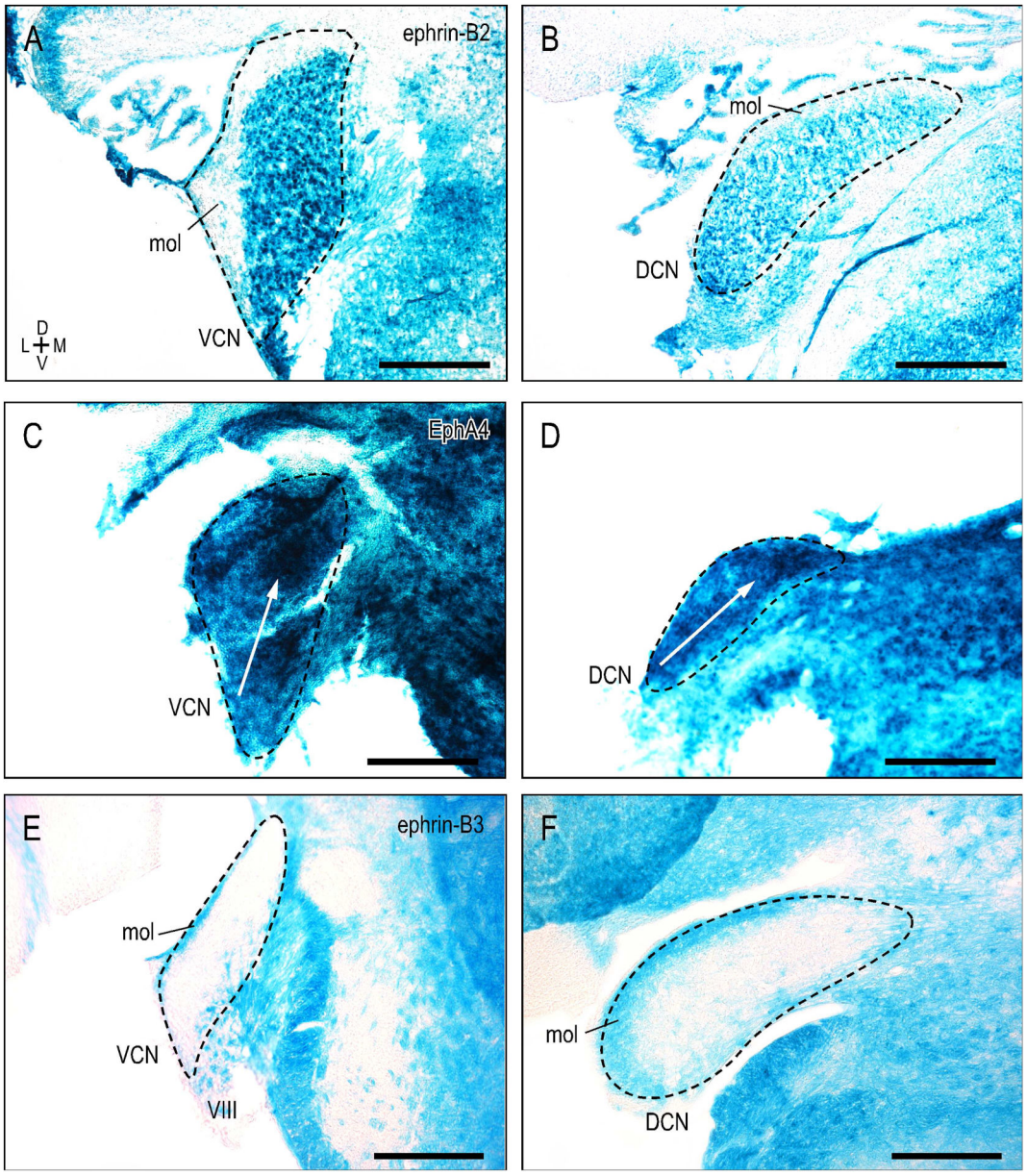

Figure 6.

Ventral and dorsal cochlear nuclei expression patterns at P4 for ephrin-B2 (A, B), EphA4 (C, D), and ephrin-B3 (E, F). Ephrin-B2 is uniformly expressed throughout the VCN and DCN, albeit lacking in the overlying molecular layer (A, B). EphA4 expression is not uniform, but graded, with protein increasingly concentrated in more dorsal, high-frequency regions (C, D; *white arrows*). Complementary to ephrin-B2, VCN and DCN are largely devoid of ephrin-B3 protein (E, F), aside from positive label confined to the molecular layer and nonuniform expression in the auditory nerve root (VIII). Dashed contours represent nuclear boundaries. Scale bars = 200 μm.

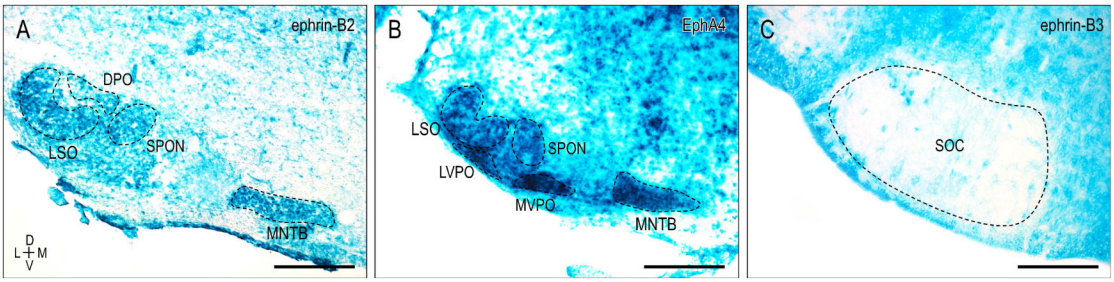

Figure 7.

X-Gal staining of the superior olivary complex (SOC) for ephrin-B2 (A), EphA4 (B), and ephrin-B3 (C) at P4. A. Ephrin-B2 is uniformly expressed throughout the LSO, SPON, MNTB, and DPO. B. EphA4 exhibits similar expression in the LSO, SPON, and MNTB, as well as prominent labeling throughout the MVPO and LVPO. C. Noteworthy ephrin-B3 expression is lacking in the early postnatal SOC. DPO = dorsal periolivary nucleus, LSO = lateral superior olivary nucleus, LVPO = lateroventral periolivary nucleus, MNTB = medial nucleus of the trapezoid body, MVPO = medioventral periolivary nucleus, SPON = superior paraolivary nucleus. Dashed contours represent nuclear boundaries. Scale bars = 200 μm.

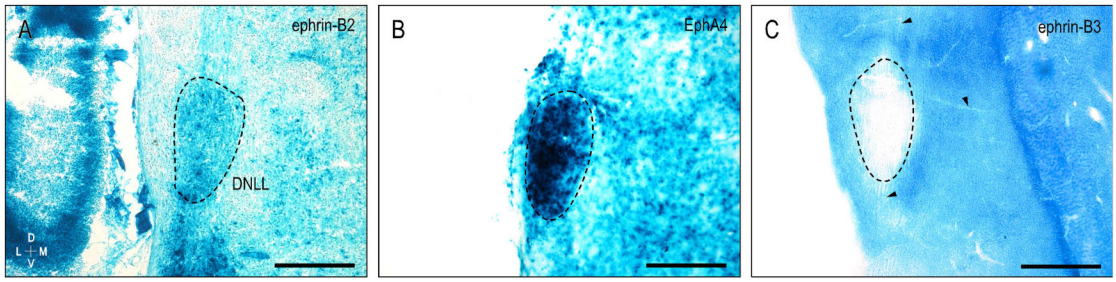

Figure 8.

Ephrin-B2 (A), EphA4 (B), and ephrin-B3 (C) expression at P8 in the dorsal nucleus of the lateral lemniscus (DNLL, *dashed contours*). Ephrin-B2 and EphA4 patterns appear complementary to ephrin-B3 labeling, which is absent from the DNLL, as well as fibers of the lateral lemniscus and commissure of Probst (*arrowheads* in C). Dashed contours denote DNLL boundaries. Scale bars = 200 μm.

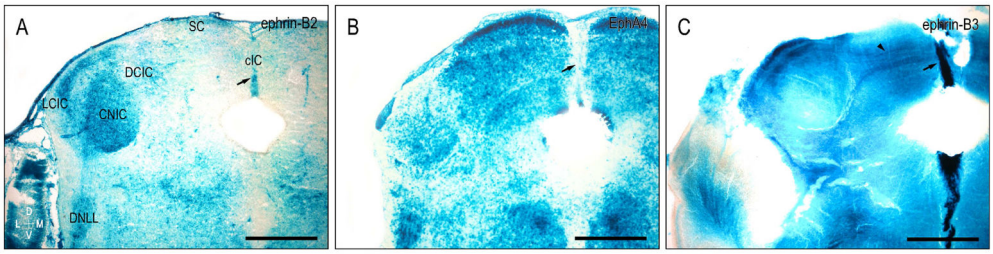

Figure 9.

Complementary midline expression of ephrin-B2 (A), EphA4 (B), and ephrin-B3 (C) at P4. The dorsal midline is ephrin-B2-positive (*arrow* in A) as is the entire midline for ephrin-B3 (*arrow* in C), while devoid of EphA4 (*arrow* in B). IC commissural fibers are consistently positive for ephrin-B3 (*arrowhead* in C). cIC = commissure of the inferior colliculus, SC = superior colliculus. Scale bars = 500 μm.

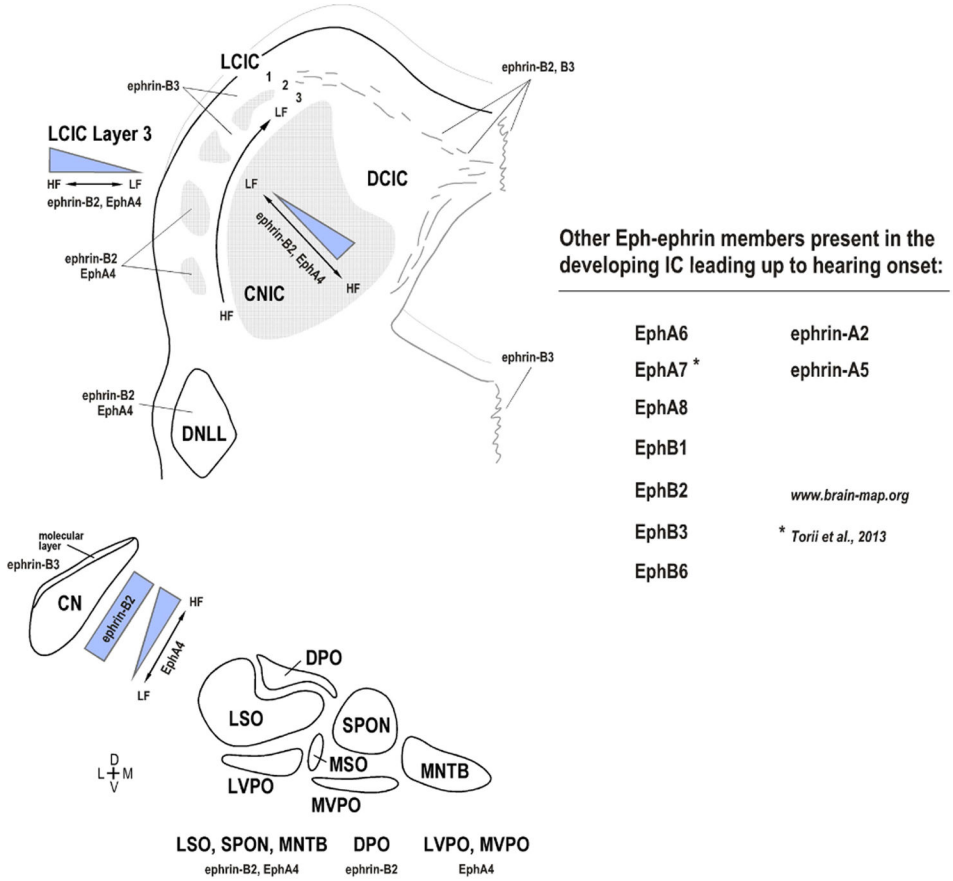

Figure 10.

Summary of ephrin-B2, EphA4, and ephrin-B3 auditory brainstem expression prior to experience. Continuous expression gradients along the tonotopic CNIC and LCIC Layer 3 are juxtaposed with discontinuous and complementary LCIC Layer 2 modular/extramodular expression. In addition to these three proteins, other members of the Eph-ephrin signaling family are likely involved in guiding continuous and discrete neural maps in the developing IC (*see* www.brain-map.org for *in situ* hybridization data). Considerable work remains identifying corresponding presynaptic guidance molecules and the precise mechanisms by which they influence IC projection mapping.